Final Report (FA4869-07-1-4087)

Nonlinear Dynamic Response Structural Optimization of a Joined-Wing Using Equivalent Static Loads

Gyung-Jin Park

Professor
Department of Mechanical Engineering
Hanyang University
1271 Sa-3 Dong, Sangnok-gu, Ansan City,
Gyeonggi-do 426-791, Korea

September 2008

Report Documentation Page

Form Approved
OMB No. 0704-0188

Public reporting burden for the collection of information is estimated to average 1 hour per response, including the time for reviewing instructions, searching existing data sources, gathering and maintaining the data needed, and completing and reviewing the collection of information. Send comments regarding this burden estimate or any other aspect of this collection of information, including suggestions for reducing this burden, to Washington Headquarters Services, Directorate for Information Operations and Reports, 1215 Jefferson Davis Highway, Suite 1204, Arlington VA 22202-4302. Respondents should be aware that notwithstanding any other provision of law, no person shall be subject to a penalty for failing to comply with a collection of information if it does not display a currently valid OMB control number.

1. REPORT DATE	2. REPORT TYPE	3. DATES COVERED
30 SEP 2008	**Final**	**06-08-2007 to 05-09-2008**

4. TITLE AND SUBTITLE
Nonlinear Dynamic Response Optimization Using the Equivalent Static Loads for a Joined-Wing

5a. CONTRACT NUMBER
FA48690714087

5b. GRANT NUMBER

5c. PROGRAM ELEMENT NUMBER

6. AUTHOR(S)
Gyung-Jin Park

5d. PROJECT NUMBER

5e. TASK NUMBER

5f. WORK UNIT NUMBER

7. PERFORMING ORGANIZATION NAME(S) AND ADDRESS(ES)
Hanyang University,1271 Sa 1-Dong, Ansan,Gyunggi-Do,South Korea,NA,426-791

8. PERFORMING ORGANIZATION REPORT NUMBER
N/A

9. SPONSORING/MONITORING AGENCY NAME(S) AND ADDRESS(ES)
AOARD, UNIT 45002, APO, AP, 96338-5002

10. SPONSOR/MONITOR'S ACRONYM(S)
AOARD

11. SPONSOR/MONITOR'S REPORT NUMBER(S)
AOARD-074087

12. DISTRIBUTION/AVAILABILITY STATEMENT
Approved for public release; distribution unlimited

13. SUPPLEMENTARY NOTES

14. ABSTRACT
The joined-wing airplane proposed by Wolkovich in 1986 is defined as an airplane that incorporates tandem wings arranged to form diamond shapes in both top and front views. The joined-wing can lead to increased aerodynamic performances as well as reduction of the structural weight. However, the joined-wing has high geometric nonlinearity under the gust load. The gust load acts as a dynamic load. In previous researches, linear dynamic response optimization and nonlinear static responses optimization are performed. In this research, nonlinear dynamic response optimization of a joined-wing is carried out by using ?equivalent static loads,? a concept expanded and newly proposed for nonlinear dynamic response optimization. Equivalent static loads are the load sets which generate the same response field in linear static analysis as that from nonlinear dynamic analysis by repeated use of linear response optimization. For the verification of efficiency of the proposed method, a simple nonlinear dynamic response optimization problem is introduced. The problem is solved by using both the equivalent static loads method and the conventional method with sensitivity analysis using the finite difference method. The procedure for nonlinear dynamic response optimization of a joined-wing using equivalent static loads is explained and the optimum results are discussed

15. SUBJECT TERMS

16. SECURITY CLASSIFICATION OF:			17. LIMITATION OF ABSTRACT	18. NUMBER OF PAGES	19a. NAME OF RESPONSIBLE PERSON
a. REPORT	b. ABSTRACT	c. THIS PAGE			
unclassified	**unclassified**	**unclassified**	**Same as Report (SAR)**	**48**	

Abstract

The joined-wing configuration that was published by Wolkovich in 1986 has been studied by many researchers. The joined-wing airplane is defined as an airplane that incorporates tandem wings arranged to form diamond shapes in both top and front views. The joined-wing can lead to increased aerodynamic performances as well as reduction of the structural weight. However, the joined-wing has high geometric nonlinearity under the gust load. The gust load acts as a dynamic load. Therefore, nonlinear dynamic (transient) behavior of the joined-wing should be considered in structural optimization. In previous researches, linear dynamic response optimization and nonlinear static responses optimization are performed. It is well known that conventional nonlinear dynamic response optimization is extremely expensive. Therefore, in this research, nonlinear dynamic response optimization of a joined-wing is carried out by using equivalent static loads. The concept of equivalent static loads is expanded and newly proposed for nonlinear dynamic response optimization. Equivalent static loads are the load sets which generate the same response field in linear static analysis as that from nonlinear dynamic analysis. Therefore, nonlinear dynamic response optimization can be conducted by repeated use of linear response optimization. For the verification of efficiency of the proposed method, a simple nonlinear dynamic response optimization problem is introduced. The problem is solved by

using both the equivalent static loads method and the conventional method with sensitivity analysis using the finite difference method. The procedure for nonlinear dynamic response optimization of a joined-wing using equivalent static loads is explained and the optimum results are discussed.

Table of Contents

LIST OF FIGURES

LIST OF TABLES

1 Introduction

The joined-wing is an innovative aircraft configuration. The joined-wing may be defined as an airplane that incorporates tandem wings arranged to form diamond shapes in both top and front views. Wolkovich proposed a joined-wing design with potential weight reduction and aerodynamic benefits as early as 1986. [1] The joined-wing has the advantage of a longer range and loiter than those of a conventional wing. Generally, the weight of the joined-wing aircraft is lighter than that of a conventional wing. Fig. 1 shows a general joined-wing aircraft where the fore-wing and aft-wing are joined. Miura, Shyu and Wolkovich employed an optimization method to study the effects of joined-wing geometry parameters on structural weight. [2] Gallman, Smith and Kroo offered many recommendations for the design methodology of a joined-wing. [3] They used the fully stressed design (FSD) for optimization. Blair and Canfield initiated nonlinear exploration on a joined-wing configuration in 2005. [4] Air Force Research Laboratories (AFRL) have been developing an airplane with a joined-wing to complete a long-endurance surveillance mission. [4-8] Lee et al. performed linear dynamic response structural optimization of a joined-wing using equivalent static loads. [9] They considered the dynamic effect of the joined-wing in optimization. In 2007, Kim et al. performed nonlinear static response optimization of a joined-wing using equivalent loads. [10]

In previous researches, [4, 10] it is certain that the joined-wing has high geometric nonlinearity under the gust loading conditions due to the specific shape of the joined-wing.

And structural optimization of the joined-wing has been performed from the viewpoint of nonlinear static response. However, real forces act dynamically. Especially, the gust loads are the most important loading conditions when an airplane wing is designed. The gust is the movement of the air in turbulence and the gust load has a large impact on the airplane. [11-12] The gust loads generate various dynamic effects on the aircraft wing. Therefore, the nonlinear dynamic effect of the joined-wing should be considered in the optimization process. However, it is very difficult to optimize a joined-wing considering the nonlinear dynamic effect. The reason is because the conventional optimization method is not efficient for nonlinear dynamic response structural optimization.

The calculation of the sensitivity from nonlinear dynamic analysis is fairly difficult. This is due to the great number of nonlinear dynamic analyses required for the calculation of the sensitivity. Therefore, the conventional gradient based optimization method is not useful for nonlinear dynamic response optimization. [13-15] The non-gradient based optimization method such as the response surface method can be used for nonlinear dynamic response optimization. However, the method has several disadvantages such as the limit of the number of design variables and inaccuracy of the solution. [16] In this research, the equivalent static loads (ESL) method is introduced for nonlinear dynamic response optimization. Until now, the equivalent static loads method has been used for linear dynamic response optimization and nonlinear static response optimization. [16-21] The concept of ESL is expanded to nonlinear dynamic response optimization.

Equivalent static loads are defined as the linear static load sets which generate the same

response field in linear static analysis as that from nonlinear dynamic analysis. Therefore, if equivalent static loads are used as applied loads, the same responses from nonlinear dynamic analysis can be considered throughout linear static response optimization. It is well known that nonlinear dynamic analysis is quite expensive. On the other hand, linear static analysis is not costly and the linear static response optimization theory is well established. Equivalent static loads are made to reduce the number of nonlinear dynamic analyses. Moreover, because the method is gradient based optimization, the solution is exact. A detailed explanation will be introduced in Section 2.

As a small example, a cantilever plate is optimized under equivalent static loads transformed from a dynamic load. The results are compared with those of a conventional method where the finite difference method is employed for sensitivity calculation. A joined-wing is optimized under dynamic gust loads. The gust loads are considered as external loads in nonlinear dynamic response optimization. The gust loads for a joined-wing have been calculated by the researchers of the AFRL. [4] Static loads for the gust can be generated from an aeroelastic model which uses the Panel method. [11-12] It is difficult to identify the exact dynamic gust load profile. Therefore, the static gust loads from AFRL are transformed to dynamic loads using the 1-cosine function. [11] ABAQUS 6.7 [24] is employed for nonlinear dynamic analysis and GENESIS 9.0 [25] is used for linear static optimization.

2 Nonlinear dynamic structural optimization using equivalent static loads (NDROESL)

As mentioned earlier, nonlinear dynamic response structural optimization is quite difficult even with the modern computer system. Nonlinear analysis considering time is a lot more expensive than nonlinear static analysis. This disadvantage is fatal for structural optimization using the gradient based optimization method because the calculation of sensitivity needs a large number of nonlinear dynamic analyses. On the other hand, the approximation methods such as the response surface method (RSM) are easy to use; however, they have a limit on the number of design variables and the solutions are not exact. [16] The equivalent static loads method is a new and efficient method that overcomes those weaknesses. In this section, the concept and the calculation of the NDROESL method are explained.

2.1 Problem formulation of nonlinear dynamic response structural optimization

The formulation for the nonlinear dynamic response optimization can be expressed as follows:

$$\text{Find} \quad \mathbf{b} \in R^m \tag{1a}$$

$$\text{to minimize} \quad f(\mathbf{b}) \tag{1b}$$

$$\text{subject to} \quad \mathbf{M(b)}\ddot{\mathbf{z}}_N(t) + \mathbf{K}_N(\mathbf{b}, \mathbf{z}_N(t))\mathbf{z}_N(t) - \mathbf{f}(t) = 0 \tag{1c}$$

$$t = 1, ..., n$$

$$g_j(\mathbf{b}, \mathbf{z}_N(t)) \le 0, \quad j = 1, \cdots, l \tag{1d}$$

$$b_{iL} \le b_i \le b_{iU}, \quad i = 1, \cdots, m \tag{1e}$$

$\mathbf{M}$ is the mass matrix which is the function of the design variable vector $\mathbf{b}$. $\mathbf{K}$ is the stiffness matrix which is the function of the design variable vector $\mathbf{b}$ and the nodal displacement vector $\mathbf{z}$, and $\ddot{\mathbf{z}}$ is the acceleration vector. The subscript N means that the response is obtained from nonlinear analysis. Eq. (1c) is the governing equation of nonlinear dynamic analysis using the finite element method. [22, 23] The constant n is the total number of the time steps. The constant l and m are the total number of the constraints and design variables, respectively. $\mathbf{f}(t)$ is the external load vector at the t th time step. b_{iL} and b_{iU} are the lower bound and upper bound of the i th design variable, respectively.

As mentioned earlier, dynamic response optimization has many time dependent constraints. As shown in Eq. (1d), the total number of time dependent constraints is $n \times l$. Moreover, the calculation of the sensitivity considering the incremental step is extremely difficult. Therefore, it is rare to perform nonlinear dynamic response structural optimization for large scale problems.

2.2 Calculation of the equivalent static loads

The equivalent static loads (ESL) are defined as the static loads which generate the same

response fields as those under a dynamic load at an arbitrary time of dynamic analysis. According to the finite element method, [22-23] the equilibrium equation of a structure in the time domain with nonlinearity is

$$\mathbf{M(b)}\ddot{\mathbf{z}}_N(t) + \mathbf{K(b}, \mathbf{z}_N(t))\mathbf{z}_N(t) = \mathbf{f}(t) \quad (t = 0,1,2,...,n) \tag{2}$$

$\mathbf{z}_N$ at all the time steps is obtained from Eq. (2). The equivalent static load for displacements is defined as:

$$\mathbf{f}_{eq}^{\mathbf{z}}(s) = \mathbf{K}_L(\mathbf{b})\mathbf{z}_N(t) \quad (s = 0,1,2,...,n) \tag{3}$$

where new notation s is exactly matched with t in Eq. (2). The reason to use the notation s is that Eq. (3) is not defined in a dynamic region but in a static region. In other words, $t = i$ is equal to $s = i$ and the total number of s is n. Therefore, n equivalent static loads are obtained from Eq. (3). $\mathbf{f}_{eq}^{\mathbf{z}}(s)$ is the equivalent load vector for displacement at each time step, $\mathbf{K}_L$ is the linear stiffness matrix and $\mathbf{z}_N(s)$ is the nodal displacement vector from Eq. (2). $\mathbf{f}_{eq}^{\mathbf{z}}(s)$ is used in Eq. (4) which is the equation of linear static analysis as follows:

$$\mathbf{K}_L(\mathbf{b})\mathbf{z}_L(s) = \mathbf{f}_{eq}^{\mathbf{z}}(s) \tag{4}$$

where the nodal displacement vector $\mathbf{z}_L(s)$ has the same values as the nonlinear nodal displacement vector $\mathbf{z}_N(t)$ in Eq. (2) at an arbitrary time. Therefore, if the equivalent static load $\mathbf{f}_{eq}^{\mathbf{z}}(s)$ is used as an external load in linear static response optimization, the same displacements as the nonlinear dynamic response can be considered in linear

response optimization. The equivalent static loads are used as multiple loading conditions for linear static response optimization and Fig. 2 presents this process.

Although the load $\mathbf{f}_{eq}^{\mathbf{z}}(s)$ can generate the same displacements as the nonlinear displacements at all the time steps, it does not generate the same stress responses because the relationships between the strain and displacement as well as the strain and stress have nonlinearity. Thus, the equivalent static loads for the stresses are separately calculated. The stress response $\boldsymbol{\sigma}_N(t)$ is obtained from Eq. (2) of nonlinear dynamic analysis. The obtained stresses are used as initial stresses of linear static analysis. The equivalent static loads for stresses are calculated as follows:

$$\mathbf{K}_L(\mathbf{b})\mathbf{z}_L^{\boldsymbol{\sigma}}(s) = -\bar{\mathbf{f}}_I(\boldsymbol{\sigma}_N(t)) \tag{5}$$

$$\mathbf{f}_{eq}^{\boldsymbol{\sigma}}(s) = \mathbf{K}_L(\mathbf{b})\mathbf{z}_L^{\boldsymbol{\sigma}}(s) \tag{6}$$

where $\mathbf{f}_{eq}^{\boldsymbol{\sigma}}(s)$ is the equivalent static load vector for the stress response, $\mathbf{K}_L$ is the linear stiffness matrix, $\boldsymbol{\sigma}_N(t)$ from Eq. (2) is utilized as the initial stress effect $-\bar{\mathbf{f}}_I(\boldsymbol{\sigma}_N(t))$ in Eq. (5) for linear static analysis. $\mathbf{z}_L^{\boldsymbol{\sigma}}(s)$ is the displacement vector from Eq. (5) and $\mathbf{f}_{eq}^{\boldsymbol{\sigma}}(s)$ is calculated by multiplying $\mathbf{K}_L$ and $\mathbf{z}_L^{\boldsymbol{\sigma}}(s)$ as shown in Eq. (6).

$\mathbf{f}_{eq}^{\boldsymbol{\sigma}}(s)$ is used as follows:

$$\mathbf{K}_L(\mathbf{b})\mathbf{z}_L(s) = \mathbf{f}_{eq}^{\boldsymbol{\sigma}}(s) \tag{7}$$

The stress response $\boldsymbol{\sigma}_L(s)$ is obtained from Eq. (7) of linear analysis. However, this stress response may not be exactly the same as that from nonlinear analysis because the

integral points for calculation of stresses are different in nonlinear dynamic analysis and the initial stress analysis. The difference can be adjusted to $\hat{\boldsymbol{\sigma}}_L(s)$ as follows:

$$\alpha_i(s) = \frac{\sigma_{Ni}(s)}{\sigma_{Li}(s)} \tag{8a}$$

$$\hat{\sigma}_{Li}^{j}(s) = \sigma_{Li}^{j}(s) \times \alpha_i(s) \tag{8b}$$

where α is the stress correction factor and i is the element number. $\sigma_{Ni}(s)$ is the nonlinear stress response from Eq. (2). $\sigma_{Li}(s)$ is the linear stress response from Eq. (7). The stress correction factor is calculated from Eq. (8a). In Eq. (8b), the superscript j means the iteration number in linear static response optimization. The corrected stress $\hat{\sigma}_{Li}^{j}(s)$ is calculated from Eq. (8b). When j is equal to zero, the corrected stress $\hat{\sigma}_{Li}^{j}(s)$ has exactly the same values as the stress response from nonlinear dynamic analysis with the initial design. The stress response $\sigma_{Li}^{j}(s)$ is changed when the design variables are changed in linear static response optimization. Because the correction factor α and the equivalent static loads $\mathbf{f}_{eq}^{\boldsymbol{\sigma}}(s)$ are constant in linear static response optimization, the corrected stress $\hat{\sigma}_{Li}^{j}(s)$ is changed as the design variables change. Ultimately, the corrected stress $\hat{\sigma}_{Li}^{j}(s)$ in linear response optimization is the same as that of the nonlinear stress response. Therefore, if the equivalent static load $\mathbf{f}_{eq}^{\boldsymbol{\sigma}}(s)$ is used as an external load with α in linear static response optimization, the same stress as the one from nonlinear analysis can be considered in the linear static response optimization process. Figure 3 presents this process.

If a problem has a displacement constraint as well as a stress constraint, equivalent loads

should be calculated with respect to each response, and the sets of the equivalent static loads are utilized in linear static response optimization as multiple loading conditions.

2.3 The steps for nonlinear dynamic response structural optimization using equivalent static loads (NDROESL)

The overall process of the NDROESL algorithm is illustrated in Fig. 4. The steps of the algorithm are as follows:

Step 1. Set initial design variables and parameters (design variables: $\mathbf{b}^{(k)} = \mathbf{b}^{(0)}$, cycle number: $k = 0$, convergence parameter: a small number ε).

Step 2. Perform nonlinear dynamic analysis with $\mathbf{b}^{(k)}$. Hence the linear stiffness matrix and nonlinear responses are obtained.

Step 3. When $k = 0$, go to Step 4. When $k > 0$, if

$$\left\| \mathbf{b}^{(k)} - \mathbf{b}^{(k-1)} \right\| \le \varepsilon \tag{9a}$$

$$g_j(\mathbf{b}^{(k+1)}, \mathbf{z}_N(t), \boldsymbol{\sigma}_N(t)) \le 0 \quad (j = 1, \cdots, l;\ t = 1, \cdots, n) \tag{9b}$$

then terminate the process. Otherwise, go to Step 4. If Eq (9a) is satisfied and Eq (9b) is not satisfied, reduce the convergence parameter ε to have a smaller value and go to Step 4.

Step 4. Calculate the equivalent static load sets as follows:

$$\mathbf{f}_{eq}^{\mathbf{z},(k)}(s) = \mathbf{K}_L(\mathbf{b})\mathbf{z}_N(t) \text{ and } \mathbf{f}_{eq}^{\boldsymbol{\sigma},(k)}(s) = \mathbf{K}_L(\mathbf{b})\mathbf{z}_L^{\boldsymbol{\sigma}}(t) \tag{10}$$

Step 5. Solve the following linear static response optimization problem:

Find $\mathbf{b}^{(k+1)}$ (11a)

to minimize $f(\mathbf{b}^{(k+1)})$ (11b)

subject to $\mathbf{K}_L(\mathbf{b}^{(k+1)})\mathbf{z}(s) - \mathbf{f}_{eq}^{\mathbf{z},(k)}(s) = 0$ (11c)

$\mathbf{K}_L(\mathbf{b}^{(k+1)})\mathbf{z}(s) - \mathbf{f}_{eq}^{\boldsymbol{\sigma},(k)}(s) = 0$ (11d)

$s = 1,...,n$

$g_j(\mathbf{b}^{(k+1)}, \mathbf{z}(s), \bar{\boldsymbol{\sigma}}(s)) \le 0, \quad j = 1,\cdots,l$ (11e)

$\mathbf{b}_{iL}^{(k+1)} \le \mathbf{b}_i^{(k+1)} \le \mathbf{b}_{iU}^{(k+1)}, \quad i = 1,\cdots,m$ (11f)

The external load $\mathbf{f}_{eq}(s)$ is the equivalent static load vector and $2n$ equivalent static load sets are used as multiple loading conditions during the linear static response optimization process.

Step 6. Update the design results, set $k = k + 1$ and go to Step 2.

2.4 A small scale example: nonlinear dynamic structural optimization of a cantilever plate

A small scale problem is solved by using the NDROESL method to validate the method. The model is a cantilever plate with 120 shell elements. The loading and boundary conditions are illustrated in Fig. 5. Figure 6(a) presents the dynamic load profile. The duration time is 0.01 second and the total analysis time is 0.1 second. ABAQUS 6.7 [24] is used for the nonlinear dynamic analysis. The implicit method is used with a constant incremental size of 0.0002. The total number of time steps is five hundred and the total

number of equivalent static loads is the same. Figure 6(b) shows the strain-stress curve of the used material for this problem. The material has bilinear elastoplastic strain-stress curve. The Young's modulus is 68.9 GPa and the tangent modulus is 34.5 GPa. The yield strength is 172 MPa. The Poisson ratio is 0.35 and the density is 2710 kg/m^3. Both geometric and material nonlinearities are considered in this problem.

Figure 7 illustrates the maximum displacement responses from nonlinear dynamic analysis and linear static analysis with ESL for the initial model. As shown, the responses are exactly the same. The maximum difference is 4x10^{-8} m. Therefore, the transformation is validated. The optimization formulation is as follows:

$$\text{Find} \quad b_i \quad (i = 1, \cdots, 29) \tag{12a}$$

$$\text{to minimize} \quad \text{Mass} \tag{12b}$$

$$\text{subject to} \quad \left|\delta_{\text{tip}}^{p}\right| \le 20.0\,\text{mm} \quad (p = 1, \cdots, 500) \tag{12b}$$

$$3.0\,\text{mm} \le b_i \le 10.0\,\text{mm} \tag{12c}$$

The design variables are the thicknesses. The cantilever plate is divided into twenty nine sections with respect to the x direction and the total number of design variables is twenty nine. The objective function is the mass. The constraint is that the magnitude of maximum displacement should be less than the allowable displacement of 20 mm at all the time steps.

This problem is solved by NDROESL as well as by a conventional method. The modified method of feasible directions algorithm in a commercial optimization code DOT 5.7 is used for the conventional method. [26] The finite difference method (FDM) is

employed for sensitivity analysis. The results of both methods are compared.

Figures 8 and 9 illustrate the history of the objective function and constraint violation for NDROESL and FDM, respectively. Table 1 shows the optimization results for the cantilever plate problem. As shown in the table, the optimum mass is almost the same. The displacement constraint is active at the optima of both methods. Figure 10 presents the maximum displacements from nonlinear dynamic analyses at the optima of both methods. They are almost the same. Since the solution from the conventional method can be considered as a mathematical optimum, the quality of the solution from NDROESL is excellent.

The efficiency of the two methods is quite different. Only eight nonlinear dynamic analyses are required in NDROESL while three hundred and sixty five analyses are required in the conventional method using FDM. The same computer, Intel Pentium Dual CPU 3.20 GHz, 3.25 GB RAM, [27] is used for the analysis and optimization. In total CPU time, NDROESL requires 22 minutes while FDM requires 486 minutes. Figure 11 illustrates the thickness distribution of the optimum models from both methods. The thickness of the root is thick and that of the tip is thin in both methods; however, the profiles are different. The difference of sensitivity causes the difference of the optimum profile. The linear response is used for the calculation of sensitivity in NDROESL. On the other hand, the nonlinear response is directly used for the calculation of sensitivity in the conventional method using FDM. The difference of sensitivity is reduced as the cycle is repeated. The results of NDROESL are almost the same as those of the conventional

method using FDM. However, NDROESL is more efficient than the conventional method.

Conceptually, it seems that the joined-wing structure is a cantilever type structure. The root of the wing is fixed at the fuselage. Several thousand shell elements are used for the finite element method of the structure. From the next section, the analysis and optimization of the joined-wing structure will be explained. Since it is a very large scale problem, the conventional method is almost impossible to use. Therefore, only the NDROESL method is used for nonlinear dynamic structural optimization of the joined-wing.

3 Analysis of the joined-wing

3.1 Finite element modeling of the joined-wing

Figure 12 illustrates a finite element model of the joined-wing. The joined-wing consists of five parts, which are the fore-wing, the aft-wing, the mid-wing, the tip-wing and the edge around the joined-wing. Each part is composed of the top skin, the bottom skin, the spar and the rib. The length from the wing-tip to the wing-root is 38 m and the length of the chord is 2.5 m. The model has 3027 elements with 2857 quadratic elements, 156 triangular elements and 14 rigid elements. Rigid elements make connections between the nodes of the aft-wing root and the center node of the aft-wing root. The structure has

two kinds of aluminum materials. One has the Young's modulus of 72.4 GPa, the shear modulus of 27.6 GPa and the density of 2770 kg/m^3. The other has 36.2 GPa, 13.8 GPa and 2770 kg/m^3, respectively. The former material is used for the entire elements except for the edge part. The latter material is only used for the elements of the edge part.

3.2 Loading conditions of the joined-wing

Eleven static loading conditions for structural optimization have been defined by the AFRL. [4] These loading conditions are composed of seven maneuver loads, two gust loads, one take-off load and one landing load as shown in Table 2. Each loading condition has a different loading direction and magnitude. The gust loading conditions are especially important in these loading conditions. Gust is the movement of the air in turbulence and the gust load has a large impact on the airplane. Static loads for the gust can be generated from an aeroelastic model which uses the Panel method. [12] The Panel method is used to calculate the velocity distribution along the surface of the airfoil. Panel methods have been developed to analyze the flow field around arbitrary bodies in two and three dimensions. The surface of the airfoil is divided into trapezoid panels. Mathematically, each panel generates the velocity on it. This velocity can be expressed by relatively simple equations which contain geometric relations, such as distances and angles between the panels. The Panel method is referred to as the boundary element method in some publications. [12] Detailed explanation of the Panel method is out of scope of this work.

The real gust load acts dynamically on the airplane. Also, dynamic loads are required for optimization with equivalent static loads. However, the generation of exact dynamic loads which consider the nonlinear dynamic behavior of the airplane is very difficult. Therefore, the static gust loads of Reference 4 are transformed to dynamic loads. Generally, there are several methods for generating dynamic gust loads. [11] Here, the approximated dynamic load is evaluated by multiplying the static load by the 1-cosine function.

The duration time of the dynamic gust load is calculated from the following equation. [11]

$$U = \frac{U_{de}}{2}\left(1 - \cos\frac{2\pi s}{25C}\right) \tag{13}$$

where U is the velocity of the gust load, U_{de} is the maximum velocity of the gust load, s is the distance penetrated into the gust and C is the geometric mean chord of the wing. The conditions for the coefficients are shown in Table 3. From Table 3 and Eq. (13), the duration time is 0.374 seconds. The airplane stays in the gust for 0.374 seconds.

The dynamic gust load is calculated as follows:

$$F_{\text{dynamic}} = F_{\text{static}} \times \left(1 - \cos\frac{2\pi}{0.374}t\right) \tag{14}$$

where F_{static} is the static gust load which is the eighth or ninth load in Table 2. It is noted that the period of the gust load is 0.374 second and the duration time of the dynamic load is 0.374 second. The dynamic load becomes zero after 0.374 second.

3.3 Boundary conditions of the joined-wing

The roots of the fore-wing and the aft-wing are joined to the fuselage. That is, the entire

part of the fore-wing root is attached to the fuselage. Therefore, all the degrees of freedom in six directions are fixed. On the other hand, the aft-wing root can be rotated with respect to the y-axis in Fig. 13. The boundary nodes of the aft-wing root are rigidly connected to the center node. The center node has an enforced rotation with respect to the y-axis. The boundary nodes are set free in the x and z translational directions. Other degrees of freedom are fixed. The enforced rotation generates torsion on the aft-wing and has quite an important aerodynamic effect. The amounts of the enforced rotation are from -0.0897 radian to 0.0 radian. These rotational values are different in each mission leg. The boundary conditions are illustrated in Fig. 13.

3.4 Nonlinear dynamic analysis of the joined-wing

Nonlinear dynamic analysis is performed under the gust loading conditions. Geometric nonlinearity is considered in nonlinear dynamic analysis. The dynamic loads are generated by Eq. (14). ABAQUS 6.7 [24] is used for nonlinear dynamic analysis. HP-UX Itanium II computer is used for nonlinear dynamic analysis [28] As mentioned before, the duration time of the dynamic gust load is 0.374 second and the total analysis time is 1.8 seconds. The size of the time step is 0.1 second. Then, the stress response is recorded every 0.1 second. Therefore, each loading condition has 18 time steps. Then, the total number of time steps is thirty six for the two gust loading conditions. In the linear static response optimization process using the equivalent static loads, thirty six static loading conditions are utilized as multiple loading conditions.

Figure 14 illustrates the von Mises stresses from nonlinear dynamic analysis. The stress fluctuates and the maximum stress occurs after 0.374 second which is the duration time of the dynamic load. Moreover, the maximum stress occurs within 1.8 seconds. Generally, the maximum stress occurs at the wing root. Figure 15 presents the stress contour of the joined-wing at 1.1 second and the maximum stress occurs under the gust loading condition 9.

4 Structural optimization of the joined-wing

4.1 Definition of design variables

As mentioned earlier, the FEM model of the joined-wing has 3027 finite elements. It is not reasonable to select the properties of all the elements as design variables for optimization. Thus, the design variable linking technology is utilized. The wing structure is divided into forty eight sections and each section has the same thickness. The finite element model is adopted from Reference 4. The joined-wing is divided into five parts as illustrated in Fig. 12. Each part is composed of the top skin, the bottom skin, the spar and the rib. Fig. 16 presents the division of the mid-wing. The top and bottom skins are divided into three sections. The sections are the wing-skin-front, the wing-skin-middle and the wing-skin-rear. The spars of the mid-wing are divided into seven sections.

The spars of other wings are divided into three sections. Other parts such as the fore-wing, the aft-wing, the wing tip and the edge are divided in the same manner. The wing tip and the edge parts are not used as design variables. Therefore, only thirty four sections among the forty eight sections are used as design variables. Design variables are defined based on Reference 9.

4.2 Optimization formulation

The optimization problem is formulated as

$$\text{Find} \quad b_i \quad (i = 1, \cdots, 34) \tag{15a}$$

$$\text{to minimize} \quad \text{Mass} \tag{15b}$$

$$\text{subject to} \quad \left|\sigma_j^p(t)\right| \le \sigma_{\text{allowable}} \tag{15c}$$

$$(p = 8,9;\ j = 1, \cdots, 1300;\ t = 1, \cdots, 18)$$

$$0.001016\,\text{m} \le b_{\text{skin part}} \le 0.05\,\text{m} \tag{15d}$$

$$0.000254\,\text{m} \le b_{\text{wing spars and ribs}} \le 0.08\,\text{m} \tag{15e}$$

where b_i is the thickness of the i th section. $\sigma_j^p(t)$ is the stress of the j th element at the t th time step under the loading condition p. As mentioned earlier, two gust loading conditions (the 8th and 9th loading conditions in Table 2) are used for nonlinear dynamic response optimization.

The objective function is the mass. The mass of the initial model is 3863 kg. The FE model has 3027 elements and each element has a different thickness. The design variables are linked according to the definition of the design variables. Then the initial

mass is 4285 kg. The upper and lower bounds are defined for each part. 0.001016 m and 0.000254 m are used as the lower bounds of the skin part and wing spars, and that of rib parts, respectively. 0.05 m is used as the upper bound of the skin part and 0.08 m is used as the upper bounds of the spars and rib parts.

The material of the joined-wing is aluminum. [4] The allowable von Mises stress for aluminum is set by 269MPa. Since the safety factor 1.5 is used, the allowable stress is reduced to 179 MPa. Stresses of all the elements except for the edge part and the wing tip part should be less than the allowable stress 179 MPa.

5 Discussion

5.1 The results of nonlinear dynamic response optimization

Nonlinear dynamic response structural optimization of the joined-wing is carried out using equivalent static loads. Two gust loading conditions are used as external dynamic loads. Each loading condition is divided into eighteen time steps from 0.0 second to 1.8 second. According to the equivalent static loads concept, thirty six static loading conditions are defined for the two gust loads.

Table 4 and Fig. 17 show the history of the optimization process. The objective function is increased by 318.4 percent from 4285.96 kg to 17933.55 kg. It is noted that the constraints are satisfied when nonlinear dynamic analysis is performed with the

optimum solution. The stress response of the optimum is illustrated in Fig. 18. The critical stresses occur at 0.2 second, 0.4 second, 0.9 second and 1.4 second. Figure 19 illustrates the stress contours of the optimum at 1.4 second. The maximum stress of optimum occurs at element 1407 which is located in the top skin of the aft-wing root. The magnitude of the maximum stress is 179.9 MPa at the time of 1.4 second. Generally, the effect of loading condition 9 (cruise speed gust load) is more severe than that of loading condition 8 (maneuver speed gust).

The violation of the stress constraint of cycle 7 is smaller than that of cycle 8. However, the mass of cycle 8 is smaller than that of cycle 7. The process is considered as converged when the difference between the design variables of the current cycle and those of the previous cycle is smaller than a given small number. The convergence criteria are satisfied in cycle 8. Both results of cycle 7 and 8 may be selected as the optimum design.

5.2 Discussion about the optimum design

As mentioned earlier, the mass is increased by 318.4 percent from 4285.96 kg to 17933.55 kg. Overall, the optimum thickness from nonlinear dynamic response structural optimization is larger than that of the initial model. In Reference 9, where linear dynamic response optimization of a joined-wing is performed, the optimum mass is 12725.52 kg. The optimum mass of nonlinear dynamic response optimization is larger than that of linear dynamic response optimization. It is reasonable because the geometric nonlinearity is added in this research. The stress constraint violation of the initial model is 344.21% in

Reference 9. However, the stress constraint violation of the initial model is 736.9% in this research. The mass of the initial design and the definition of the design variables are not exactly the same between Reference 9 and this research. However, the FEM model, the boundary conditions and the critical loading conditions are the same. Therefore, it seems that this comparison is useful for the design of a joined-wing.

Table 5 and Fig. 20 show the optimum thickness. The thicknesses of the parts in the aft-wing are quite large. The leading edge and middle part of the top skin, the trailing edge part of the bottom skin and the leading and trailing spars of the aft-wing are as thick as the upper bounds. In Fig. 20, dv$i$ means the design variable number. In the top skin of the aft-wing, the thicknesses of the leading edge and middle section are larger than that of the trailing edge. On the other hand, in the bottom skin of the aft-wing, the thickness of the trailing edge is larger than that of the leading edge. This means that a large torsion force occurs at the aft-wing root position. This torsion effect is observed in Fig. 19. In the top skin of the aft-wing root, a large stress occurs at the leading edge. At the bottom skin of the aft-wing root, a large stress occurs at the trailing edge. It seems that the optimum thicknesses of the aft-wing are influenced by the torsion effect.

6 Conclusions

The joined-wing is defined as an airplane that incorporates tandem wings arranged to form diamond shapes in both top and front views. The joined-wing configuration has many advantages from the viewpoint of aerodynamic performance and weight reduction. However, due to the specific shape of the joined-wing, it has large geometric nonlinearity under the gust loading conditions. The real gust acts dynamically. Therefore, the nonlinear dynamic behavior should be considered in structural optimization of a joined-wing. The dynamic gust load profile is calculated by multiplying the static gust loads by the 1-cosine function.

The equivalent static loads are used for nonlinear dynamic response structural optimization of a joined-wing. The existing concepts of the equivalent static loads are expanded for nonlinear dynamic response optimization. This is called nonlinear dynamic response optimization using equivalent static loads. (NDROESL) The equivalent static loads are defined as the linear static load sets which generate the same response field in linear static analysis as that from nonlinear dynamic analysis. Therefore, if equivalent static loads are used as applied loads, the same responses from nonlinear dynamic analysis can be considered in linear static response optimization. Equivalent static loads are made to reduce the number of nonlinear dynamic analyses. Also, because the method is gradient based optimization, the solution is exact. An example of the cantilever plate is solved by NDROESL as well as the conventional method using the finite difference method. By comparing results, NDROESL is more efficient than the conventional method. And the objective function values of the two methods are almost the same.

The optimum design considering the nonlinear dynamic effect of the joined-wing satisfies all the stress constraints. The joined-wing is divided into forty eight sections and the thicknesses of thirty four sections are used as design variables for nonlinear dynamic response optimization. The mass is increased by 318.4 percent. It is because the constraint violation of the initial model is quite large and the thicknesses of almost all the sections are increased. It is noted that the optimum thicknesses of the leading edge of the top skin and those of the trailing edge of the bottom skin in the aft-wing are 5 cm, which is the upper bound. Only eight nonlinear dynamic analyses are required for nonlinear dynamic response structural optimization of the joined-wing. Nonlinear dynamic response optimization of a joined-wing using the proposed method is very successful and efficient although the problem is fairly large scale.

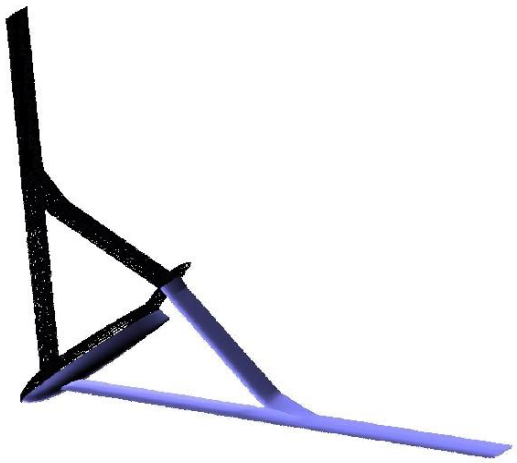

Fig. 1 Configuration of the joined-wing

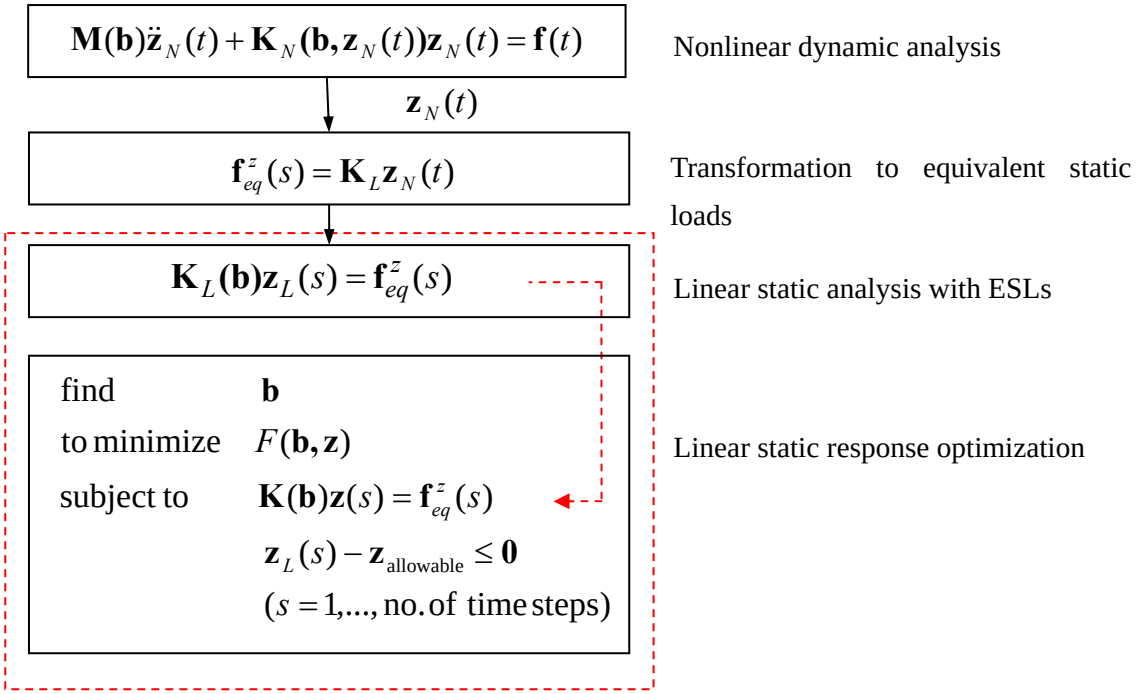

Fig. 2 Generation of equivalent static loads for displacement constraints

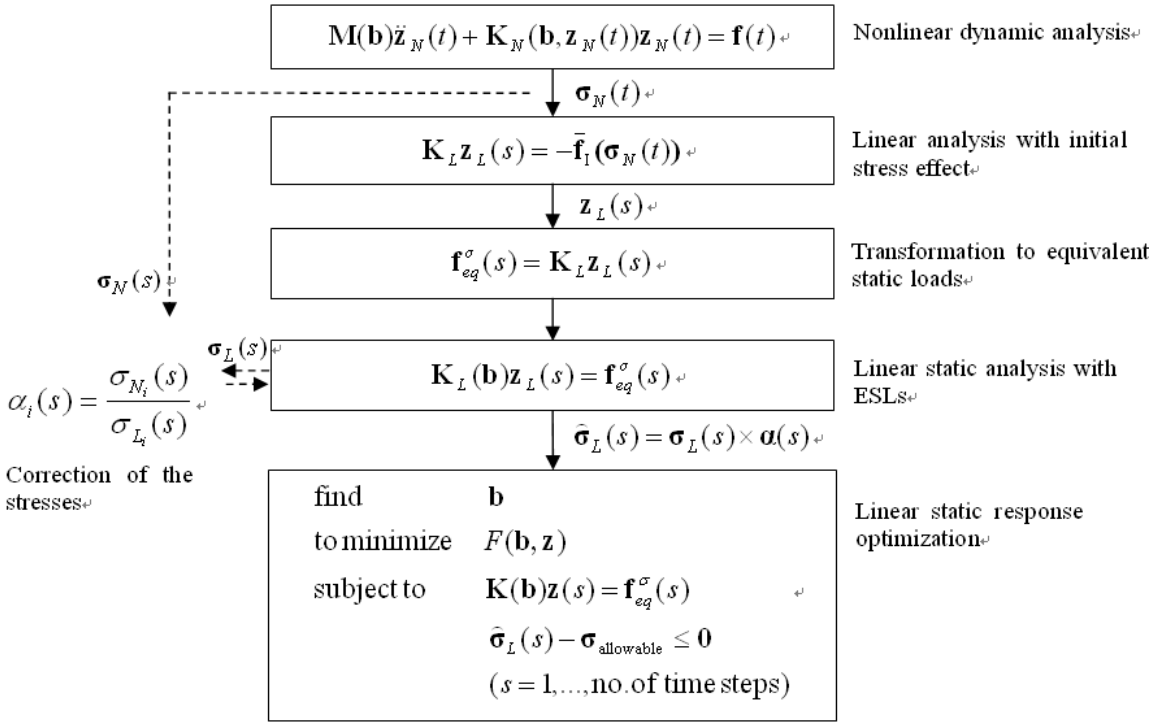

Fig. 3 Generation of equivalent static loads for stress constraints

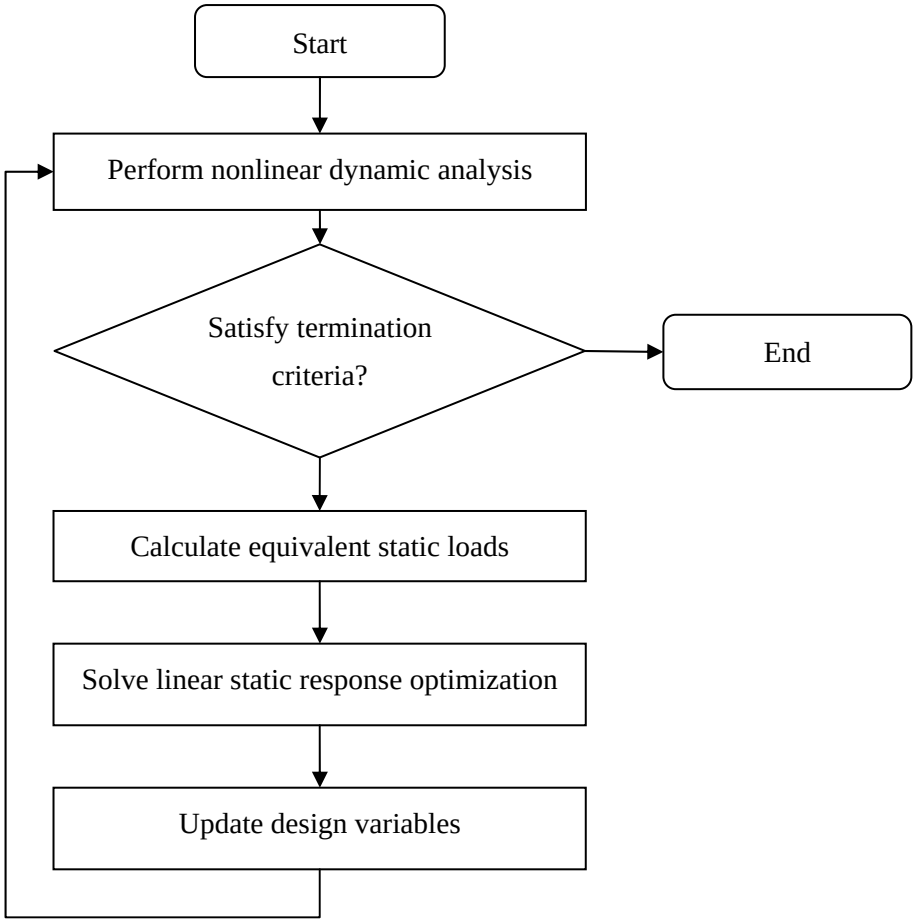

Fig. 4 Optimization process using the equivalent static loads

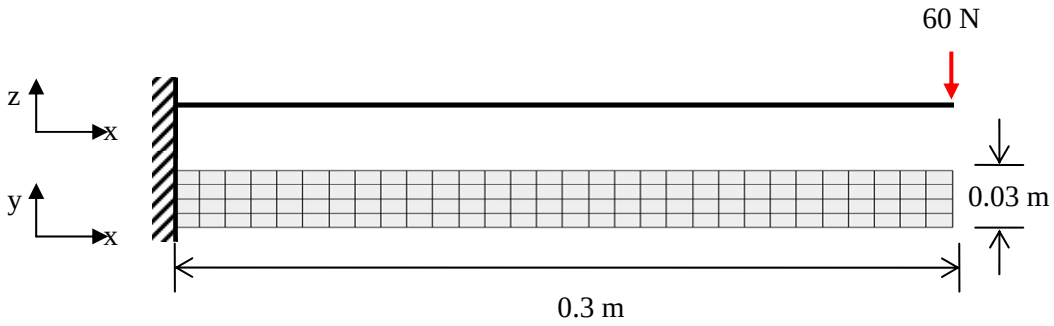

Fig. 5 Cantilever plate structure

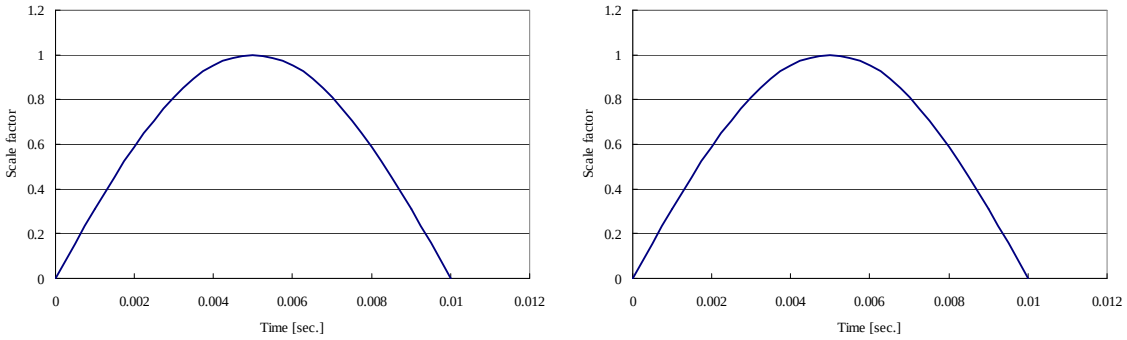

(a) Dynamic load profile of the cantilever plate structure

(b) Bilinear elastoplastic strain-stress curve

Fig. 6 Dynamic load profile and strain-stress curve of the cantilever plate structure.

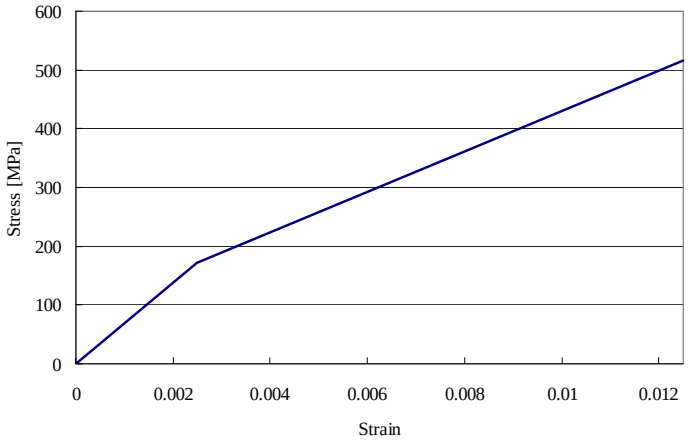

Fig. 7 Displacement response from nonlinear dynamic analysis and linear static analysis with ESL for the initial model

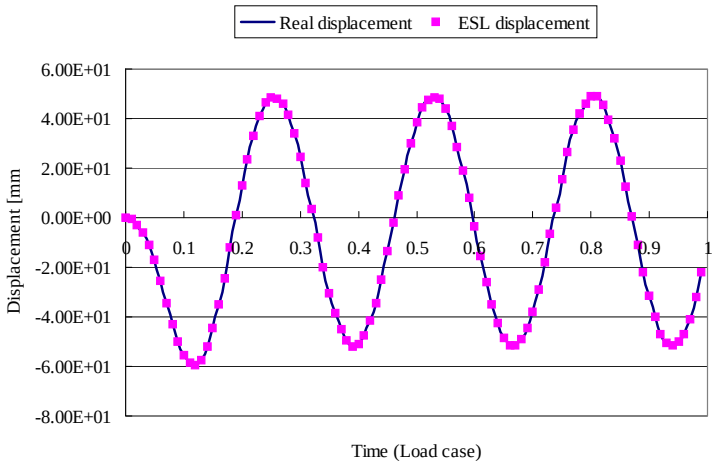

Fig. 8 Objective function and constraint violation history of the cantilever plate structure using NDROESL

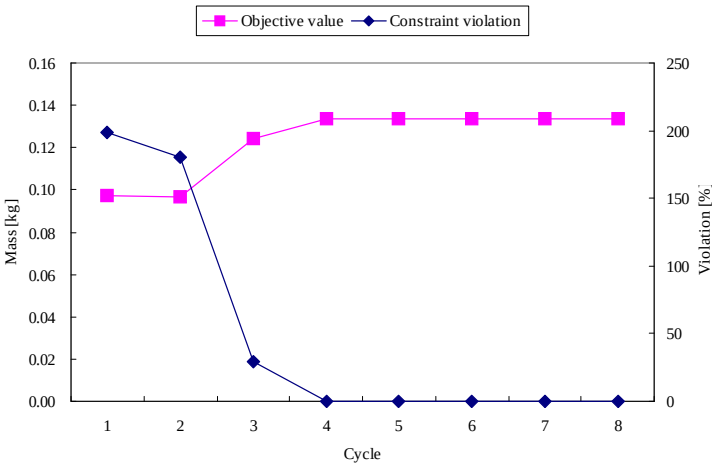

Fig. 9 Objective function and constraint violation history of the cantilever plate structure using FDM

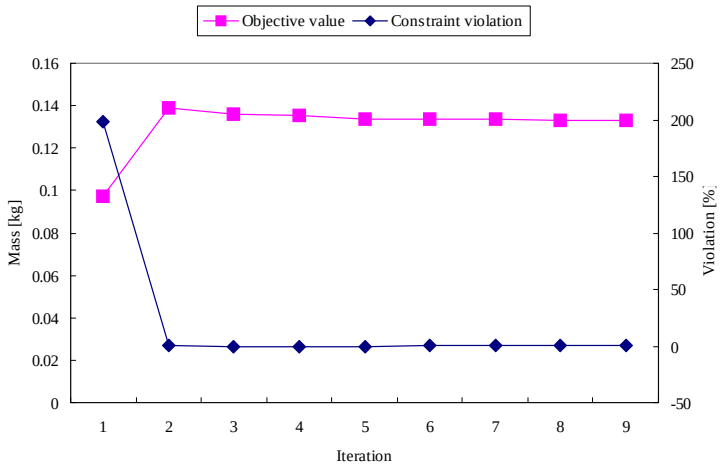

Fig. 10 Displacement response from nonlinear dynamic analysis with optimum design of NDROESL and FDM

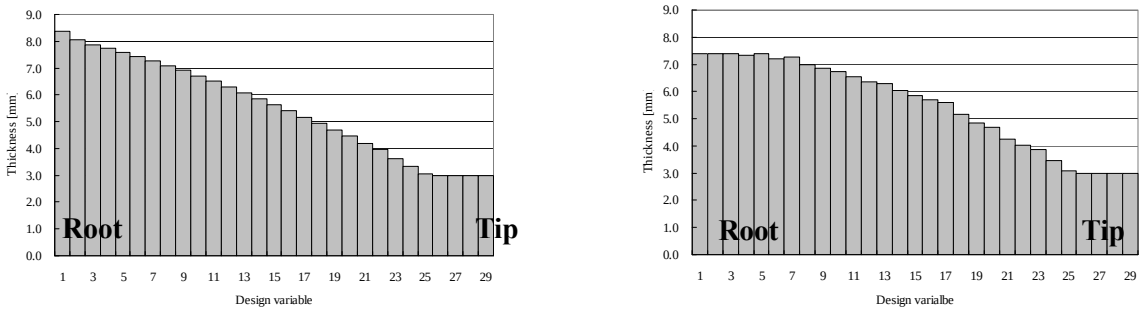

(a)NDROESL result (b) FDM result

Fig. 11 Thickness distribution of the optimum models from NDROESL and FDM

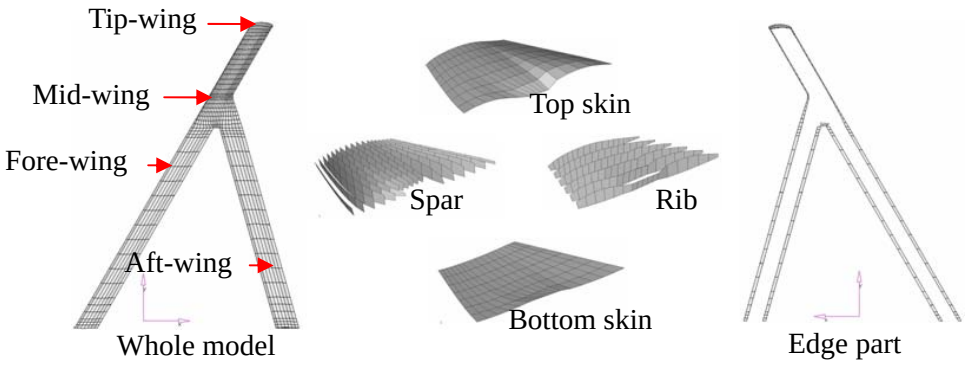

Fig. 12 Finite element modeling of the joined-wing

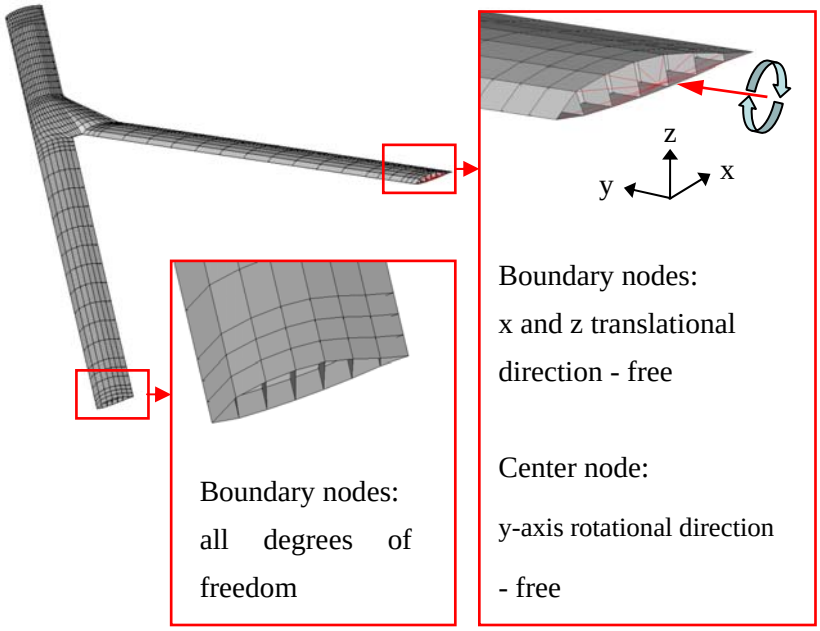

Fig. 13 Boundary conditions of the joined-wing

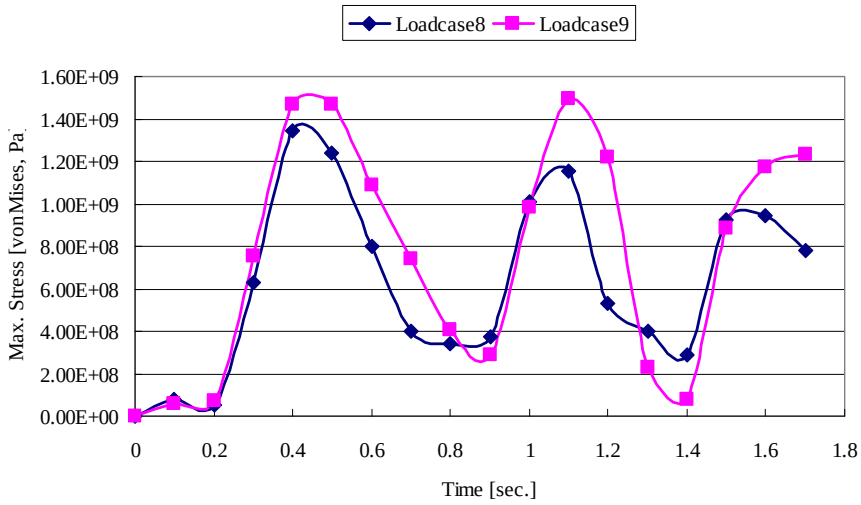

Fig. 14 Stress response of the joined-wing under the cruise speed gust loading condition

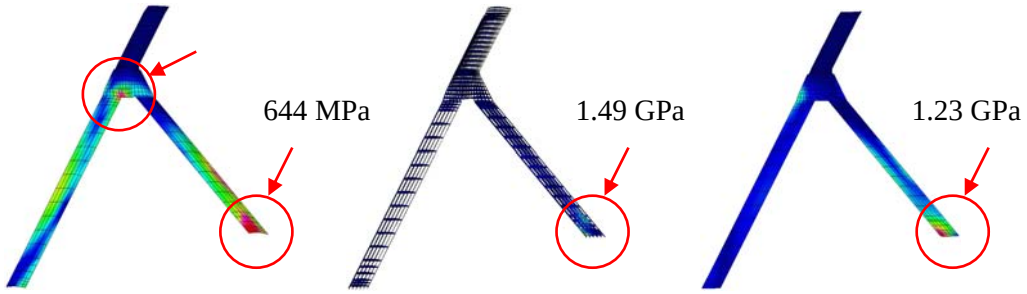

(a) Top skin (b) Rib and spar (c) Bottom skin

Fig. 15 Stress contours at 1.1 second from nonlinear dynamic analysis of a joined-wing

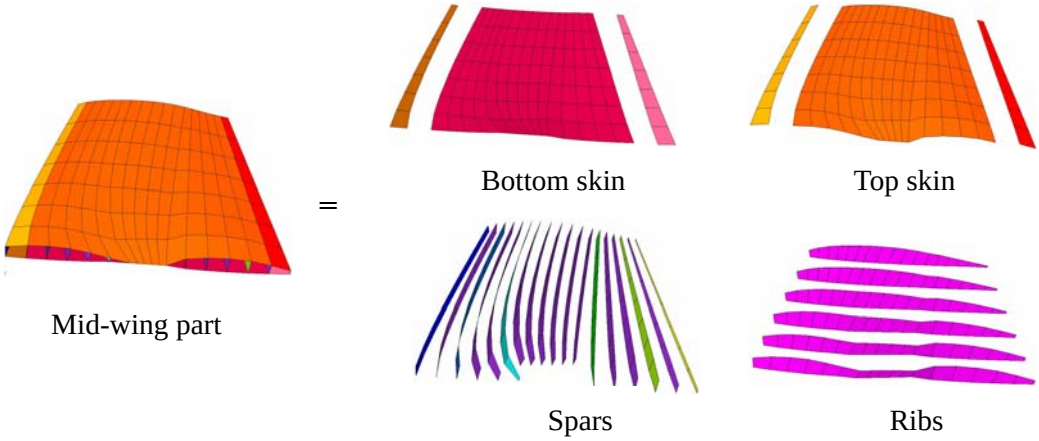

Fig. 16 Sections for definition of design variables

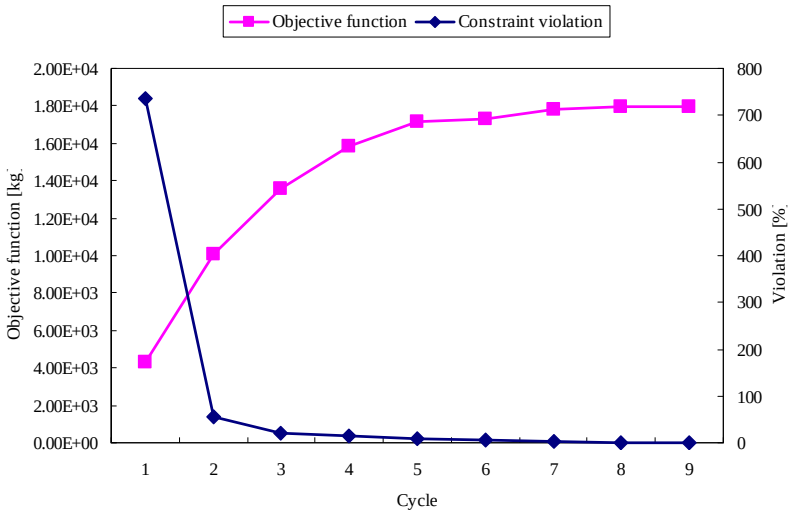

Fig. 17 History of nonlinear dynamic response structural optimization

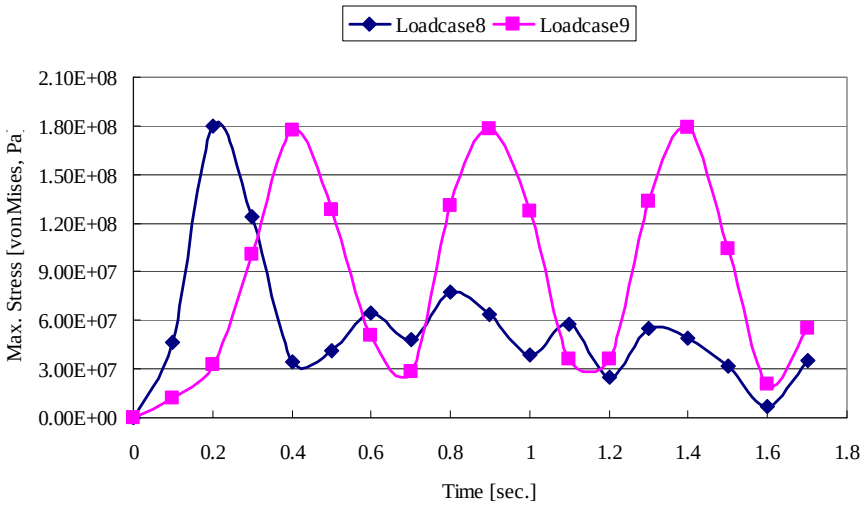

Fig. 18 Stress response of the optimum design under the cruise speed gust loading condition

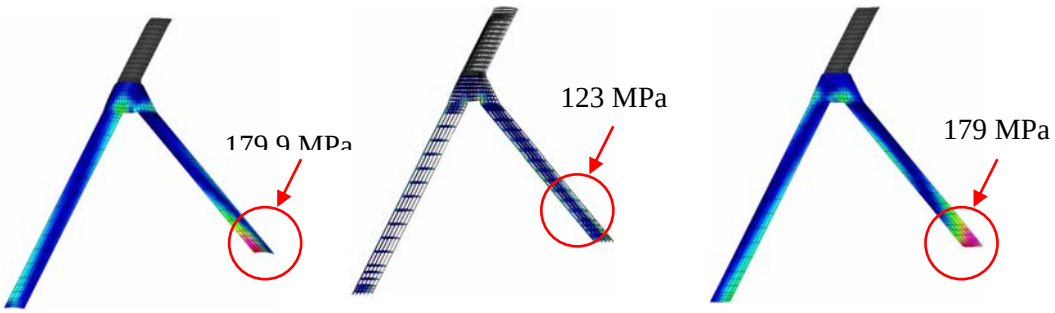

(a) Top skin (b) Rib and spar (c) Bottom skin

Fig. 19 Stress contours of the optimum design at 1.4 second

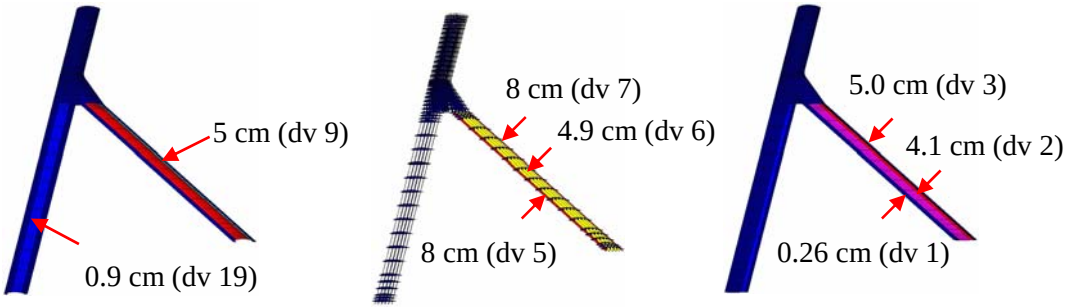

(a) Top skin (b) Rib and spar (c) Bottom skin

Fig. 20 Thickness contour of the nonlinear dynamic response optimization result

Table 1 Optimum results for the cantilever plate problem

	Initial	Optimum of NDROESL	Optimum of FDM
Mass	0.09756 kg	0.13353 kg	0.13314 kg
Maximum displacement	59.6 mm	20.00 mm	20.06 mm
Number of iterations (cycles)		8	9
Number of nonlinear transient analyses		8	365
Number of nonlinear transient analyses except for gradient call			104
Total number of iterations for linear response optimization		24	
Total CPU time		22 minutes	486 minutes

Table 2 Load data of the joined-wing

Number of loading condition	Load type	Mission leg
1	2.5 g PullUp	Ingress
2	2.5 g PullUp	Ingress
3	2.5 g PullUp	Loiter
4	2.5 g PullUp	Loiter
5	2.5 g PullUp	Egress
6	2.5 g PullUp	Egress
7	2.5 g PullUp	Egress
8	Gust (Maneuver)	Descent
9	Gust (Cruise)	Descent
10	Taxi (1.75 g impact)	Take-off
11	Impact (3.0 g landing)	Landing

Table 3 Aerodynamic data for the joined-wing

Gust maximum velocity	18.2 m/s
Flight velocity	167 m/s
Geometric mean chord of wing	2.5 m
Distance penetrated into gust	62.5 m

Table 4 Results of nonlinear dynamic response optimization of the joined-wing

Iteration no.	Optimum value (kg)	Constraint violation (%)
0	4285.96	736.9
1	10078.70	54.2
2	13608.93	19.8
3	15857.66	15.0
4	17129.80	8.9
5	17326.98	6.7
6	17797.18	2.3
7	17944.14	0.0
8	17933.55	0.5

Table 5 Optimum thicknesses from nonlinear response optimization using ESL

Number	Name	Initial thickness (meter)	Optimum thickness (meter)
1	AFT_BOTTOM_SKIN_FRONT	0.001020	0.002626
2	AFT_BOTTOM_SKIN_MIDDLE	0.001554	0.040679
3	AFT_BOTTOM_SKIN_REAR	0.023830	0.049995
4	AFT_RIB	0.000298	0.010910
5	AFT_SPAR_FRONT	0.000288	0.079995
6	AFT_SPAR_MIDDLE	0.000798	0.048723
7	AFT_SPAR_REAR	0.080000	0.079995
8	AFT_TOP_SKIN_FRONT	0.041890	0.049995
9	AFT_TOP_SKIN_MIDDLE	0.002718	0.049996
10	AFT_TOP_SKIN_REAR	0.001493	0.017102
11	FORE_BOTTOM_SKIN_FRONT	0.001442	0.005083
12	FORE_BOTTOM_SKIN_MIDDLE	0.003319	0.006304
13	FORE_BOTTOM_SKIN_REAR	0.009598	0.013159
14	FORE_RIB	0.000274	0.000356
15	FORE_SPAR_FRONT	0.000615	0.000479
16	FORE_SPAR_MIDDLE	0.000732	0.001265
17	FORE_SPAR_REAR	0.012790	0.009565
18	FORE_TOP_SKIN_FRONT	0.002578	0.003251

19	FORE_TOP_SKIN_MIDDLE	0.004656	0.009070
20	FORE_TOP_SKIN_REAR	0.001539	0.003532
21	MID_BOTTOM_SKIN_FRONT	0.001020	0.004202
22	MID_BOTTOM_SKIN_MIDDLE	0.002000	0.003295
23	MID_BOTTOM_SKIN_REAR	0.001261	0.002538
24	MID_RIB	0.000384	0.001997
25	MID_SPAR	0.000838	0.000398
26	MID_SPAR1	0.000254	0.001663
27	MID_SPAR2	0.000254	0.000254
28	MID_SPAR3	0.000254	0.000254
29	MID_SPAR4	0.000542	0.003763
30	MID_SPAR5	0.000254	0.000339
31	MID_SPAR6	0.000458	0.016899
32	MID_TOP_SKIN_FRONT	0.001020	0.005426
33	MID_TOP_SKIN_MIDDLE	0.001793	0.004075
34	MID_TOP_SKIN_REAR	0.001020	0.001090

References

1. Wolkovich, J., "The Joined-Wing: An Overview," *Journal of Aircraft*, Vol. 23, No. 3, 1986, pp. 161-178.
2. Miura, H., Shyu, A. T. and Wolkovich, J., "Parametric Weight Evaluation of Joined Wings by Structural Optimization," *Journal of Aircraft*, Vol. 25, No. 12, 1988, pp. 1142-1149.
3. Gallman, J. W., and Kroo, I. M., "Structural Optimization of Joined-Wing Synthesis," *Journal of Aircraft*, Vol. 33, No. 1, 1996, pp. 214-223.
4. Blair, M., Canfield, R. A., and Roberts, R. W., "Joined-Wing Aeroelastic Design with Geometric Nonlinearity," *Journal of Aircraft*, Vol. 42, No. 4, 2005, pp. 832-848.
5. Blair, M., and Canfield, R. A., "A Joined-Wing Structural Weight Modeling Study," *AIAA/ASME/ASCE/AHS/ASC Structures, Structural Dynamics, and Materials Conference*, AIAA, Denver, CO, 2002.
6. Roberts, R. W., Canfield, R. A., and Blair, M., "Sensor-Craft Structural Optimization and Analytical Certification," *AIAA/ASME/ASCE/AHS/ASC Structures, Structural Dynamics, and Materials Conference*, AIAA, Norfolk, VA, 2003.
7. Rasmussen, C. C., Canfield, R. A., and Blair, M., "Joined-Wing Sensor-Craft Configuration Design," *AIAA/ASME/ASCE/AHS/ASC Structures, Structural Dynamics, and Materials Conference*, AIAA, Palm Springs, CA, 2004.
8. Rasmussen, C. C., Canfield, R. A., and Blair, M., "Optimization Process for Configuration of Flexible Joined-Wing," *AIAA/ISSMO Multidisciplinary Analysis and Optimization Conference*, AIAA, Albany, NY, 2004.
9. Lee, H. A., Kim, Y. I., Park, G. J., Kolonay, R. M., Blair, M. and Canfield, R. A., "Structural Optimization of a Joined-Wing Using Equivalent Static Loads," *Journal of Aircraft*, Vol. 44, No. 4, 2007, pp. 1302-1308.
10. Kim, Y. I., Park, G. J., Kolonay, R. M., Blair, M. and Canfield, R. A., "Nonlinear Response Structural Optimization of a Joined-Wing Using Equivalent Loads," *7th World Congress on Structural and Multidisciplinary Optimization*, WCSMO7, Seoul, Korea, 2007.
11. Hoblit, F. M., *Gust Loads on Aircraft: Concepts and Applications*, American Institute of Aeronautics and Astronautics, Inc., Washington, DC, 1988, Chaps. 2, 3.

12. Katz, J., Plotkin, A., *Low-Speed Aerodynamics*, McGraw-Hill, NY, 1991.
13. Haftka, R. T. and Gürdal, Z. *Elements of Structural Optimization*, Kluwer Academic Publishers, Netherlands, 1992.
14. Arora, J. S., *Introduction to Optimum Design, International edition*, McGraw-Hill Book Co., Singapore, 2001.
15. Kim, N. H. and Choi, K., K., "Design Sensitivity Analysis and Optimization of Nonlinear Transient Dynamics," *Mechanics Based Design of Structures and Machines,* Vol. 29, No. 3, 2001, pp. 351-371.
16. Park, G. J., *Analytical Methods in Design Practice*, Springer, Germany, 2007.
17. Choi, W. S., and Park, G. J., "Structural Optimization Using Equivalent Static Loads at All the Time Intervals," *Computer Methods in Applied Mechanics and Engineering*, Vol. 191, No. 19, 2002, pp. 2077-2094.
18. Kang, B. S., Choi, W. S., and Park, G. J., "Structural Optimization Under Equivalent Static Loads Transformed from Dynamic Loads Based on Displacement," *Computers and Structures*, Vol. 79, No. 2, 2001, pp. 145-154.
19. Park, G. J., and Kang, B. S., "Validation of a Structural Optimization Algorithm Transforming Dynamic Loads into Equivalent Static Loads," *Journal of Optimization Theory and Applications*, Vol. 118, No. 1, 2003, pp. 191-200.
20. Shin, M. K., Park, K. J. and Park, G. J., "Optimization of Structures with Nonlinear Behavior using Equivalent Loads," *Computer Methods in Applied Mechanics and Engineering*, Vol. 196, 2007, pp. 1154-1167.
21. Kim, Y. I., Lee, H. A. and Park, G. J, "Case Studies of Nonlinear Response Structural Optimization using Equivalent Loads," *The Fourth China-Japan-Korea Joint Symposium on Optimization of Structural and Mechanical Systems*, CJKOSM4, Kunming, China, 2006.
22. Cook, R. D., Malkus, D. S., Plesha, M. E. and Witt, R. J., *Concepts and Applications of Finite Element Analysis, fourth edition*, John Wiley and Sons. Inc., NY, 2001.
23. Bathe, K. J., *Finite Element Procedures*, Prentice-Hall, Inc., New Jersey, 1996.
24. ABAQUS/Standard Version 6.7, User's Manual, Hibbitt, Karlsson and Sorensen, Inc. Pawtucket, RI, USA, 2004.
25. GENESIS User's Manual, Version 9.0, Vanderplaats Research and Development,

Inc., Colorado Springs, CO, 2005.

26. DOT User's Manual, Version 5.7, Vanderplaats Research and Development, Inc., Colorado Springs, CO, 2001.

27. Intel Corporation, http://www.intel.com/products/chipsets/index.htm [cited 14 December 2007]

28. Hewlett-Packard Development Company, L. P., URL: http://www.testdrive.hp.com/current.shtml [cited 20 March 2007]